EFFECT OF NONLINEARITIES ON THE TRANSIENT RESPONSE OF AN ELECTROHYDRAULIC POSITION CONTROL SERVO

Ahmed Abo-Ismail, Assiut University, Egypt
Asok Ray, The Pennsylvania State University

The analysis and design of hydraulic servosystems are often based on linear models that are suitable for inputs of small amplitude [References 1 and 2]. Linear models or linearized versions of nonlinear models may not accurately represent the servosystem characteristics when the system is subject to inputs of large amplitude, such as those encountered in ON–OFF control. The impact of the nonlinearities of the dynamic response and stability of the system needs to be clarified.

Davies, et al. [Reference 3] have studied the harmonic response of an electrohydraulic servomechanism where a jump resonance phenomenon was predicted, and its cause was determined to be the pressure/flow nonlinearity. The Coulomb-friction was included in the analysis, while valve dynamics were neglected. Martin [Reference 4] clarified the effect of valve saturation on the step response of a hydraulic servo with mechanical feedback and a single-stage spool valve, where the effects of Coulomb-friction and valve dynamics were neglected. Nikiforuk, et al. [Reference 5] studied the transient response of a time-optimized hydraulic servomechanism operating under cavitation conditions and where the actuator displacement was determined graphically over a limited range of time values. Vilenius [Reference 6] presented a nonlinear model to simulate the dynamics of an electrohydraulic stepping motor, and predicted the angular deflection of motor shaft only, where the influence of Coulomb-friction was neglected.

Abo-Ismail, et al. [Reference 7] clarified the effect of the pressure/flow nonlinearity on the step response of a hydraulic servomechanism employing a single-stage nozzle-flapper valve. However, Coulomb-friction and valve dynamics were not included in the analysis. Ray [Reference 8] studied the effects of inertia of fluid and mechanical parts on the dynamic performance of a hydraulic relief valve. In this investigation, the nonlinear characteristics of the valve were represented by an empirical relationship obtained from the manufacturer's specifications.

Shearer [Reference 9] presented an extensive study for digital simulation of a Coulomb-damped hydraulic servosystem employing nonlinear valve characteristics. The output velocity and load pressure were predicted for an alternating ramp input. However, it was indicated that the transient oscillation of the model died out more quickly than the real system did when Coulomb-friction was present. Moreover, while the simulated results were periodic and symmetric in nature; the experimental results were not. Watton [Reference 10] applied the method of characteristics to determine the transient response of a speed control system, which was dominated by the fluid inertia in long hydraulic lines (up to a length of 10.73 m). Moreover, the effects of oil compressibility and load viscous friction were not included in the analysis.

The objective of this paper is to present a nonlinear mathematical model which allows simulation and analysis of the dynamic characteristics of an electrohydraulic position control servo. In the dynamic simulation model, two major nonlinearities are considered: (1) pressure/flow characteristics associated with the spool valve, and (2) Coulomb-friction, which is already present or intentionally introduced in the valve motor load. The model includes valve dynamics as well as the effects of oil compressibility and actuator leakage. Responses for the angular displacement of motor shaft and load pressure due to large amplitude step input are obtained by digital simulation. The dynamics of the servosystem with position feedback as well as with velocity feedback are simulated. The simulation results are found to be in agreement with the experimental data that were generated under similar operational environments and input disturbances.

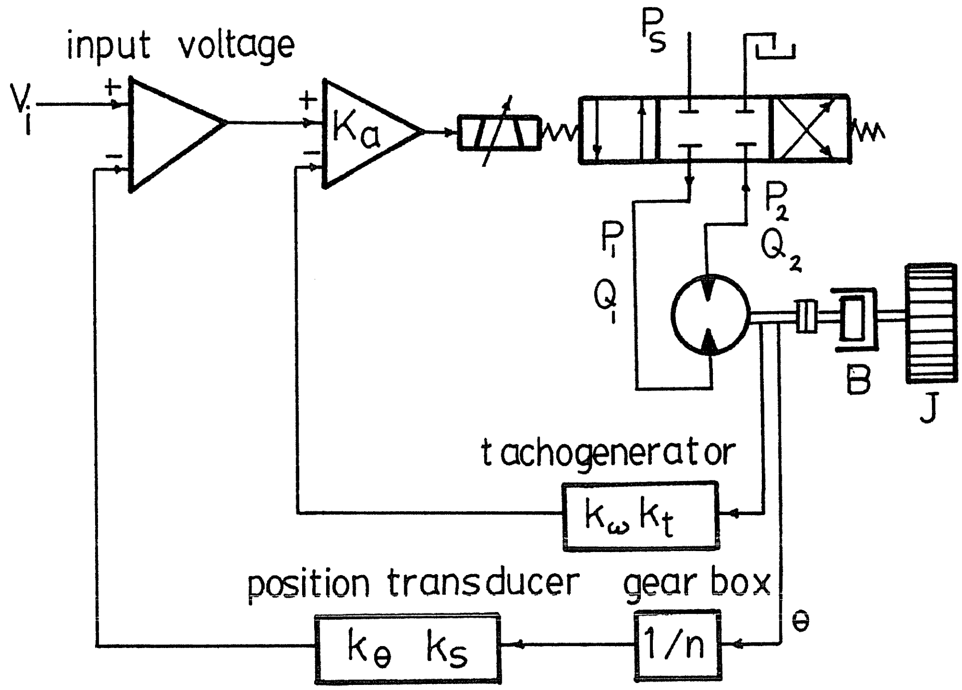

Figure 1. Schematic Diagram of the Servosystem

The paper is organized into six sections and two appendices. A brief description of the electrohydraulic servosystem is given in the following section "System Description." Analytical expressions for the nonlinear valve model and the equations for the simulation model are presented in sections "Nonlinear Model" and "Computer Simulation Model," respectively. The results obtained from simulation and experimentation are discussed in "Results and Discussion." The conclusions derived from this research work as well as recommendations for future research are given in the final section. Appendices I and II provide the details of the steady-state and dynamic models of the valve, respectively.

System Description

The closed-loop electrohydraulic position control system under consideration is shown schematically in Figure 1. A two-stage electrohydraulic servovalve is connected to a hydraulic rotary actuator by very short high pressure hoses. The closed-loop action is obtained by comparing the angular position of the motor shaft with the input signal by a synchro error channel. This forms the major loop. A tachogenerator is used to measure the angular velocity, which can be used as a feedback signal to the input of the servovalve drive amplifier. This forms a minor loop.

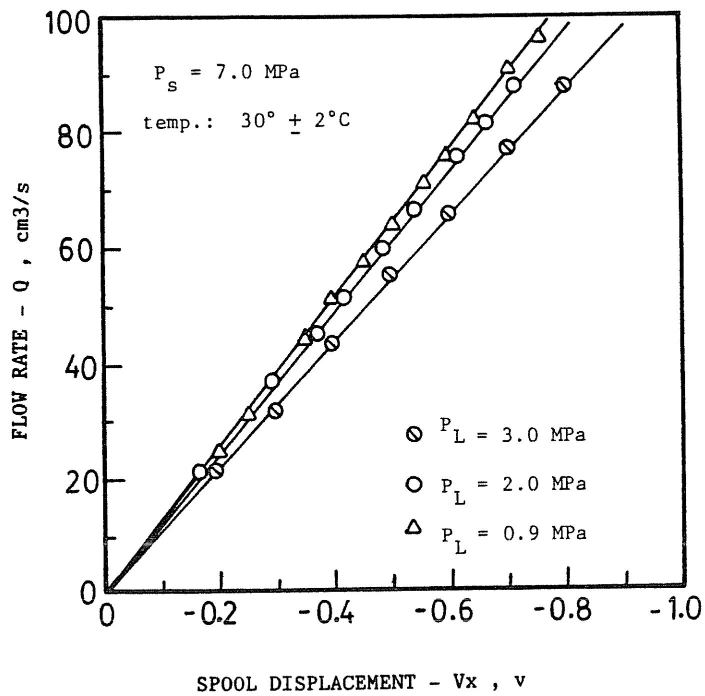

Figure 2. Valve Flow–Gain

The electrohydraulic valve consists of a first-stage nozzle-flapper valve, and a second-stage 4-way spool valve. The valve drive amplifier has a gain of 100 mA/V. The valve is of the zero-lap type, as seen from the valve flow gain at different load pressures shown in Figure 2. The steady-state pressure/flow performance of the servovalve was modeled using the experimental data as shown in Figure 3.

Nonlinear Model

The model is derived on the assumption that an inertially loaded rotary motor is controlled by a two-stage electrohydraulic servovalve (see Figure 1). In this analysis, the nonlinearity of the pressure-flow characteristics of the servovalve is attributed to the second-stage spool valve, and the valve dynamics are assigned to the first-stage nozzle-flapper valve.

The steady-state valve model as derived in Appendix I is represented by the following relation

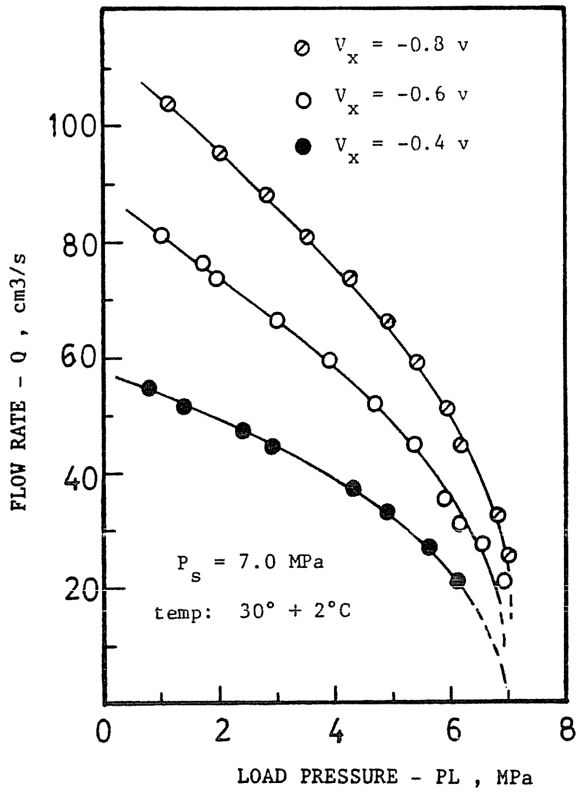

Figure 3. Pressure/Flow Characteristics

$$Q = K_x V_x \operatorname{sgn}\left[1 - (\operatorname{sgn} V_x)\frac{P_L}{P_s}\right]\sqrt{\left|1 - (\operatorname{sgn} V_x)\frac{P_L}{P_s}\right|} \tag{1}$$

where Q is the volumetric flowrate through the valve, P_L is the load pressure, P_s is the supply pressure, K_x is the valve gain, and V_x is the valve input voltage.

The dynamic performance of the servovalve is described by a first-order time lag (see Appendix II), and is given by

$$\tau\frac{dQ}{dt} + Q = K_x V_x \tag{2}$$

where τ is the valve time constant.

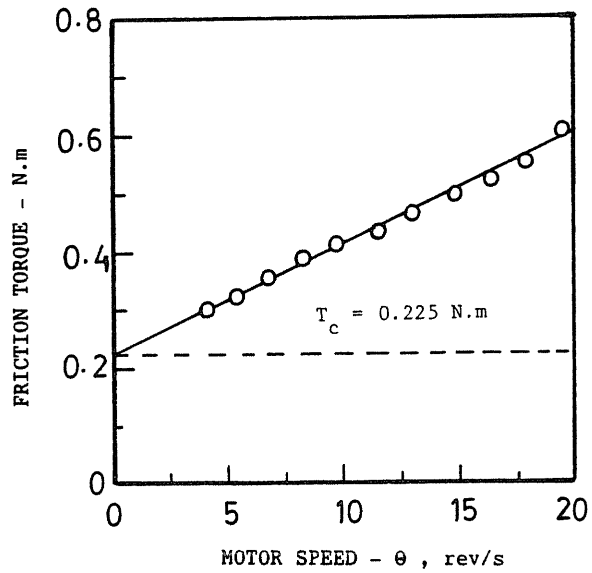

Figure 4. Motor Friction Losses

Equations 1 and 2 are combined to yield a dynamic valve model as

$$\tau \frac{dQ}{dt} + Q = K_x V_x \operatorname{sgn}\left[1 - (\operatorname{sgn} V_x)\right] \sqrt{\left|1 - (\operatorname{sgn} V_x)\frac{P_L}{P_s}\right|} \tag{3}$$

The hydraulic motor is modeled by considering the rotary motor arrangement shown in Figure 1, as well as by taking into account oil compressibility and leakage across the motor. Using the principle of conservation of mass yields

$$Q = V_m \frac{d\theta}{dt} + \frac{V_c}{4K_h}\frac{dP_L}{dt} + L_e P_L \tag{4}$$

where θ is the angular displacement of the motor shaft, V_m is the motor displacement/rad, V_c is the volume of oil in motor hoses, K_h is the hydraulic bulk modulus and L_e is the effective leakage coefficient.

The load characteristics of the motor were formulated from the experimentally obtained data for friction losses as given in Figure 4. The results exhibit the existence of Coulomb-friction in addition to the viscous friction. Thus the equation of motion of the load is given by

$$P_L V_m = J\frac{d^2\theta}{dt^2} + B\frac{d\theta}{dt} + T_c \operatorname{sgn}\dot{\theta} \tag{5}$$

where J is the inertia of load and rotating parts, B is the viscous damping coefficient and T_c is the magnitude of the Coulomb-friction torque.

The feedback transducers and operational amplifier were modeled as follows:

A synchro error channel was used to sense the position of the hydraulic motor shaft, compare it to the input signal and derive an error signal. This forms the major feedback loop which is described as

$$e_p = V_i(t) - \frac{k_\theta k_s \theta}{n} \tag{6}$$

where e_p is the error signal, $V_i(t)$ is the disturbing reference voltage, k_θ is the position feedback gain, k_s is the displacement transducer constant, θ is the angular position of the shaft and n is the reduction gear ratio.

The velocity feedback is generated by using a tachogenerator which derives a voltage signal and feeds it back to a differential amplifier, thus forming the minor loop. This action is given by

$$e_v = e_p - k_\omega k_t \frac{d\theta}{dt} \tag{7}$$

where e_v is the actuating error signal, k_ω is the velocity feedback gain and k_t is the tachogenerator constant.

The action of the operational amplifier, which has a gain range of ± 3 is given by

$$V_x = e_v K_a \tag{8}$$

where V_x is the servovalve drive voltage and K_a is the operational amplifier gain.

Computer Simulation Model

Definition of the state variables and inputs of the system are given below:

States:

$$\begin{aligned} x_1 &= \theta(t) \\ x_2 &= \dot{\theta}(t) \\ x_3 &= P_L(t) \\ x_4 &= \dot{P}_L(t) \end{aligned}$$

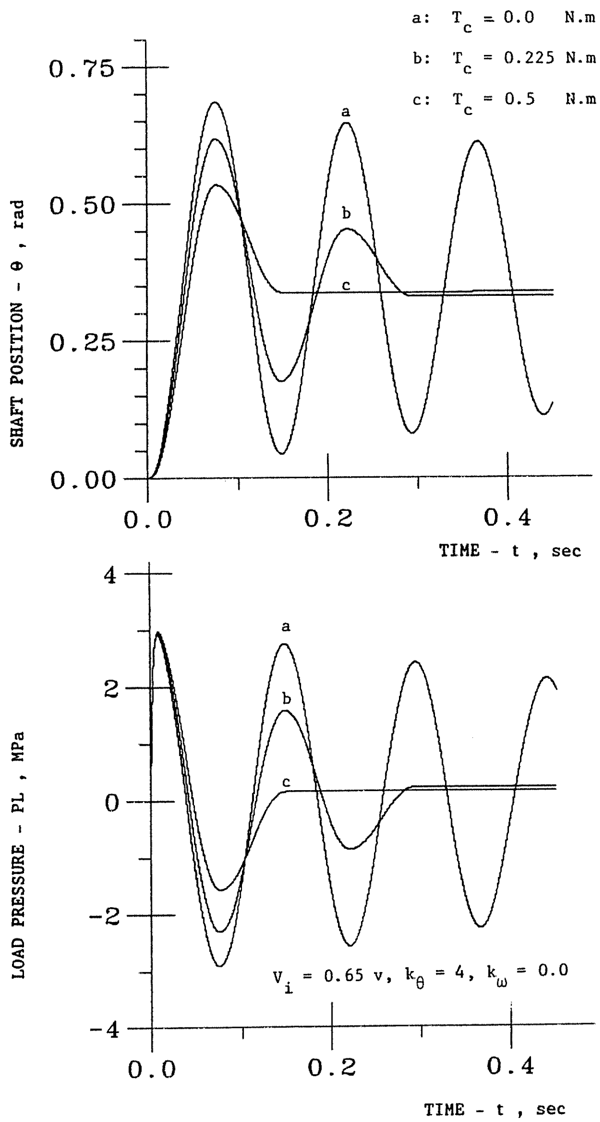

Figure 5. Influence of Coulomb-Friction on Servo Response

Inputs:

$$u_1 = V_i(t)$$
$$u_2 = P_s \tag{9}$$

Applying the states definition to the system of nonlinear equations (1–8), after manipulation, results in the state variable model as follows:

$$\dot{x}_1 = x_2 \tag{10}$$

$$\dot{x}_2 = -\frac{B}{J}x_2 + \frac{V_m}{J}x_3 - \frac{T_c}{J}\operatorname{sgn} x_2 \tag{11}$$

$$\dot{x}_3 = x_4 \tag{12}$$

$$\begin{aligned}
\dot{x}_4 = &-x_1\left[\frac{4K_h}{\tau V_c}\frac{K_xK_ak_\theta k_s}{n}\operatorname{sgn}\left\{1-(\operatorname{sgn}V_x)\frac{x_3}{u_2}\right\}\sqrt{\left|1-(\operatorname{sgn}V_x)\frac{x_3}{u_2}\right|}\right] \\
&+x_2\left[\frac{4K_h}{\tau V_c}\left(\frac{\tau V_m B}{J} - V_m - K_xK_ak_\omega k_t\operatorname{sgn}\left\{1-(\operatorname{sgn}V_x)\frac{x_3}{u_2}\right\}\sqrt{\left|1-(\operatorname{sgn}V_x)\frac{x_3}{u_2}\right|}\right)\right] \\
&-x_3\left[\frac{4K_hV_m^2}{JV_c} + \frac{4K_hL_e}{\tau V_c}\right] - x_4\left[\frac{1}{\tau} + \frac{4K_hL_e}{V_c}\right] \\
&+\frac{4K_hV_m}{JV_c}T_c\operatorname{sgn} x_2 \\
&+\left(\frac{4K_h}{\tau V_c}\right)K_xK_au_1\operatorname{sgn}\left\{1-(\operatorname{sgn}V_x)\frac{x_3}{u_2}\right\}\sqrt{\left|1-(\operatorname{sgn}V_x)\frac{x_3}{u_2}\right|}
\end{aligned} \tag{13}$$

The state-variable model represented by equations (10–13) is of the nonlinear form

$$\dot{x}(t) = f[x(t), u(t)] \tag{14}$$

The initial conditions of the state variables are given by:

$$\begin{aligned}
x_1(0) &= 0 \\
x_2(0) &= 0 \\
x_3(0) &= 0 \\
x_4(0) &= 0
\end{aligned} \tag{15}$$

The parameters of the system appearing in the state-variable model, Equation 14, are given in Table 1.

A digital simulation program was used to evaluate the system output, namely the angular position of motor shaft and the corresponding load pressure for large amplitude step input. The simulation program was executed at The Pennsylvania State University on a VAX-11/780 computer, while the experimental work was carried out at the Mechanical Engineering Department of Assiut University, Egypt.

Valve:	
τ, valve time constant (s)	2.3×10^{-3}
V_i, valve drive voltage (v)	0.65
K_a, operational amplifier gain	-1
K_x, valve steady-state gain at P_L=0(m^3/s/v)	-1.36×10^{-4}
P_s, supply pressure (N/m^2)	7×10^6
Motor:	
V_c, volume of oil in motor and hoses (m^3)	20.5×10^{-6}
V_m, motor displacement (m^3/rad)	0.716×10^{-6}
L_e, equivalent leakage coefficient (m^5/N.s)	2.8×10^{-11}
K_h, hydraulic bulk modulus (N/m^2)	1.4×10^9
Load:	
B, viscous damping coefficient (N.m.s/rad)	2.95×10^{-3}
J, motor inertia (N.m.s^2/rad)	3.4×10^{-3}
T_c, magnitude of Coulomb-friction (N.m)	0.225
Transducers:	
k_t, tachogenerator constant (v/rad/s)	0.026
k_s, position transducer constant (v/rad)	3.44
k_Θ, position feedback gain	4
k_ω, velocity feedback gain	1
n, reduction gear ratio	7.5

Table 1. System Parameters

Results and Discussion

The effects of Coulomb-friction and pressure/flow nonlinearities on dynamic performance, and stability of the closed loop electrohydraulic servosystem with position feedback were demonstrated by simulation. The results of simulation are presented as a series of curves in Figures 5 to 10. The transient responses of shaft angular position and load pressure for step disturbances in the reference position signal are illustrated.

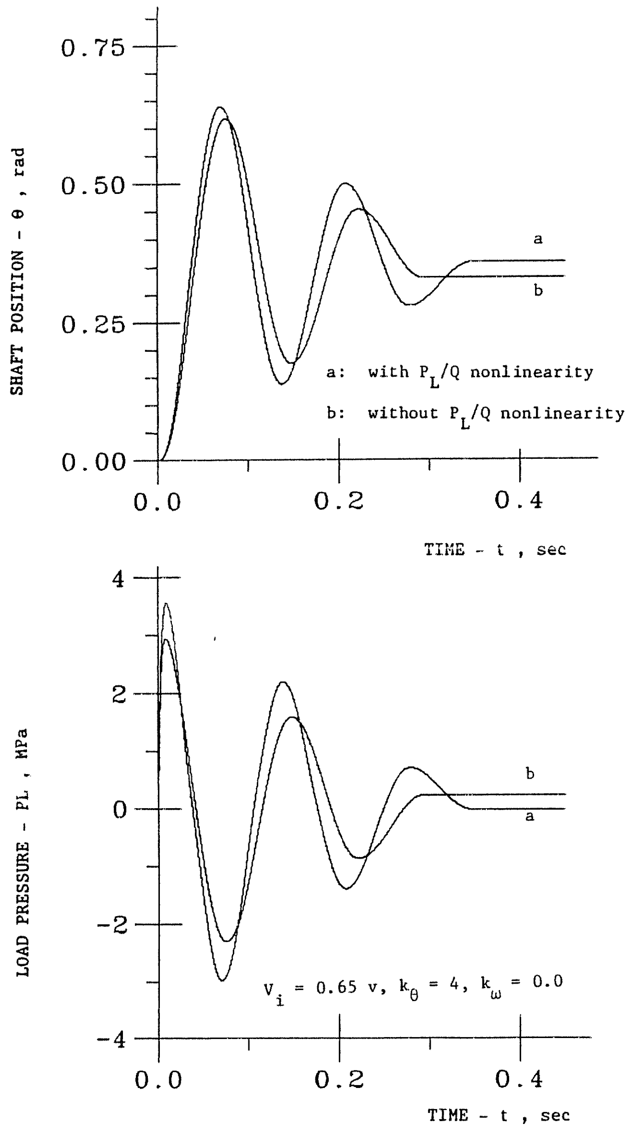

Figure 6. Influence of Pressure/Flow Nonlinearity on Servo Response

The simulated responses were obtained by applying a step increase in the reference input signal from a steady-state condition with different magnitudes of Coulomb-friction at 0.000, 0.225 N·m and 0.500 N·m. Simulation results are shown in Figure 5 for shaft angular position and load pressure with position feedback—the effects of pressure/flow nonlinearity were not included in this case in order to observe the effects of Coulomb-friction more clearly. It is demonstrated that as the magnitude of Coulomb-friction is increased from 0.225 N·m to 0.5 N·m, the dynamic response was remarkably improved in the sense that number of oscillations was reduced and settling time was decreased from 0.3 to 0.15 seconds approximately. On the other hand, when Coulomb-friction was neglected, the response showed an excessive number of oscillations due to very low damping. This behavior is not normally acceptable for practical applications.

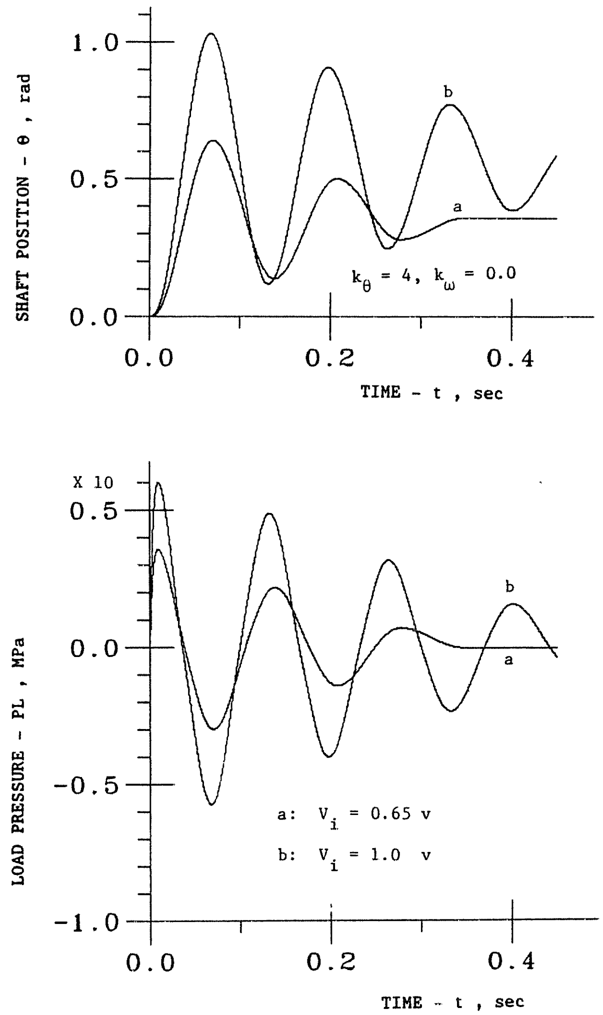

Figure 7. Influence of Input Amplitude on Servo Response

Figure 6 presents simulation results for the transient response of the angular position of the motor shaft and load pressure when both the pressure/flow nonlinearity and Coulomb-friction (with $T_c = 0.225$ N·m) are taken into account. Curves a and b in Figure 6 indicate the response with and without the effects of pressure/flow nonlinearity in the simulation model, respectively. Comparison of curves a and b in Figure 6 indicates that the pressure/flow nonlinearity tends to reduce the dynamic response due to an increased number of oscillations and larger overshoot. Correspondingly, the settling time is increased from 0.3 seconds in case b to 0.35 seconds in case a.

This shows that a simplified model that neglects pressure/flow nonlinearities could generate inaccurate results. The load pressure response indicates that the servosystem is characterized by a very high pressure sensitivity at the initiation of the disturbance. This is, indeed, required for providing an adequate torque for motor motion.

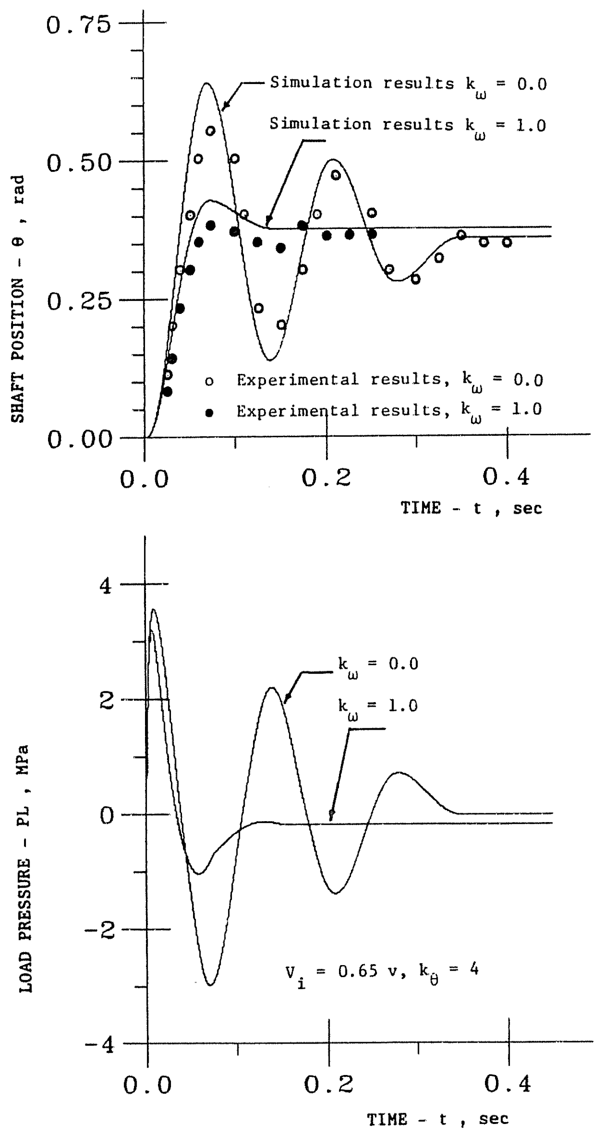

Figure 8. Influence of Velocity Feedback on Servo Response, $V_i = 0.65$ v

The simulated response of the system to two different amplitudes of step disturbances in the reference input signal, $V_i = 0.65$ volt and $V_i = 1.0$ volt, is shown in Figure 7 (as indicated by curves a and b, respectively). The response with $V_i = 1.0$ volt is more oscillatory with increased overshoot, and correspondingly, it takes a longer time for the transients to die out. Even with this large amplitude input, the system does not exhibit cavitation, since the maximum value of the overshoot in P_L is less than the supply pressure, $P_s =$ 7.0 MPa.

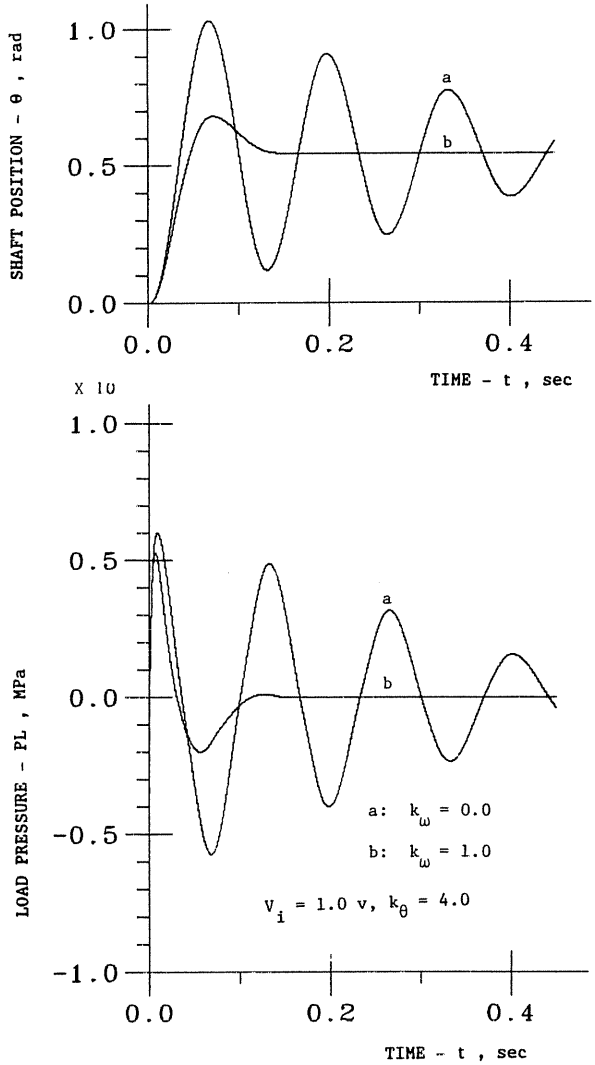

Figure 9. Influence of Velocity Feedback on Servo Response, $V_i = 1.0$ v

In order to investigate the effects of a minor loop compensation on the servosystem performance, a velocity feedback was applied with a gain of $k_\omega = 1$ in addition to the position- feedback with a corresponding gain of $K_\theta = 4$. Results of the transient response of the velocity-compensated servosystem are shown together with the results of the uncompensated system ($K_w = 0$) in Figures 8 and 9 for the reference input amplitudes of $V_i = 0.65$ volt and $V_i = 1.0$ volt, respectively. The responses shown in Figures 8 and 9 highlight the important role played by the velocity feedback. The settling time is considerably decreased, and is practically independent of the input disturbance amplitude. Furthermore the response is appropriately damped. This indicates that a combination of position and velocity feedback can significantly improve the dynamic response of a hydraulic servosystem.

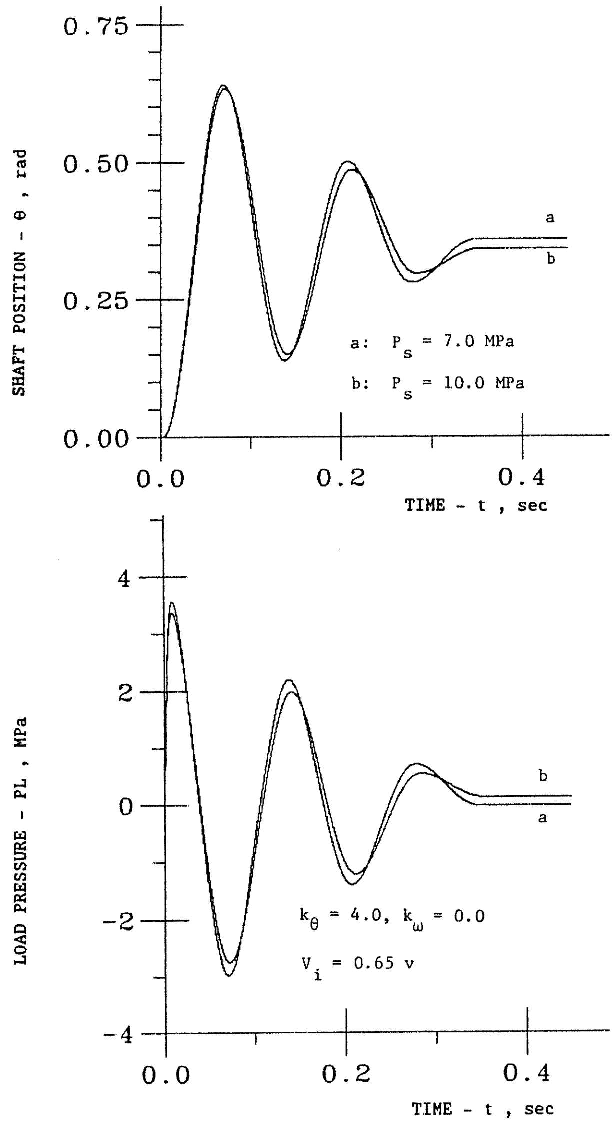

Figure 10. Influence of Supply Pressure on Servo Response

Experimental results of the output shaft position with the reference input amplitude of $V_i = 0.65$ volt are also given in Figure 8. The speed of response, namely the settling time, and the steady-state position for both experimental and simulated results are found to be in close agreement. However the experimental results are characterized by a smaller overshoot with and without velocity feedback, as shown in Figure 8. These discrepancies could be attributed to the lag effects in the transmission lines as well as in the recording instruments, which were not included in the simulation model.

All results presented so far in this analysis were obtained with a supply pressure of 7.0 MPa. In order to investigate the effects of variations in supply pressure, such as due to the faulty operation of a relief valve, the response of the servosystem was obtained with supply pressures of 7.0 MPa and 10.0 MPa as represented by curves a and b in Figure 10. A comparison of the curves a and b indicates that the damping effect increases with a rise in supply pressure. However, it was observed from other simulation results obtained during this study that small variations in the supply pressure of the order of 10 percent would have negligible effect on the system response.

Conclusions and Recommendations for Future Work

The effects of Coulomb-friction and pressure/flow nonlinearities on the transient response of electrohydraulic position control servosystems have been investigated. A nonlinear dynamic model of the closed-loop servosystem was developed for simulating its transient and steady-state behavior under different operational scenarios. The results obtained from the simulation model are in agreement with the experimental data.

Results of the simulation show that the transient response of the closed-loop servosystem could be effectively damped if velocity feedback is used in conjunction with position feedback. However, velocity feedback requires additional instrumentation. In the absence of a velocity feedback signal, dynamic response could still be effectively damped if Coulomb-friction is introduced in the valve motor load. In this case, the system may not be asymptotically stable, i.e., there may be a steady-state position error. Thus, the dead band in Coulomb-friction should be determined on the basis of a trade-off between dynamic and steady-state performance of the closed-loop servo control system.

The next generation of hydraulic servosystem is expected to implement advanced control algorithms that will take advantage of the computational capabilities of dedicated microcomputers [References 11 and 12]. In this respect, other control strategies such as variable structure control (VSS) [Reference 13] that could improve both dynamic and steady-state performance should be investigated.

It is observed that the pressure/flow nonlinearity tends to make the system response more oscillatory and increase the settling time. Therefore, the effects of pressure/flow nonlinearity should not be neglected for servovalve control system design. Simulation results also indicate that there is no evidence of cavitation under large perturbations in the reference input, even if only position feedback is in effect.

References

1. D. McCloy and H. R. Martin. *Control of Fluid Power*, 2nd (revised) edition, Wiley/Ellis Horwood Ltd., 1980.
2. J. F. Blackburn, G. Reethof and J. L. Shearer. *Fluid Power Control*, Cambridge MA: MIT Press, 1960.
3. A. M. Davies and R. M. Davies. "Nonlinear Behavior, Including Jump Response, of Hydraulic Servomechanisms," *Journal of Mechanical Engineering Science*, Vol. 11, No. 3, 1969, pp. 281–289.
4. K. F. Martin. "Flow Saturated Step Response of a Hydraulic Servo," *Transactions of the ASME, Journal of Dynamic Systems, Measurement, and Control*, September 1974, pp. 341–346.
5. P. N. Nikiforuk, J. N. Wilson and R. M. Lepp. "Transient Response of a Time-Optimized Hydraulic Servomechanism Operating Under Cavitation Conditions," *Proc. Instn. Mech. Engrs.*, Vol. 185, 1970-71, pp. 837–846.
6. M. J. Vilenius. "Dynamics of an Electrohydraulic Stepping Motor," *Transactions of the ASME, Journal of Dynamic Systems, Measurement, and Control*, March 1977, pp. 63- 65.
7. Ahmed Abo-Ismail, et al. "Step Response of a Hydraulic Servo-mechanism," *Proc. of the International Symposium on Fluid Control and Measurement*, September 1985, Tokyo, Japan.
8. A. Ray. "Modeling and Simulation of a Relief Valve," *Simulation*, November 1978, pp. 167–172.
9. J. L. Shearer. "Digital Simulation of a Coulomb-Damped Hydraulic Servosystem," *Transactions of the ASME, Journal of Dynamic Systems, Measurement and Control*, Vol. 105, December 1983, pp. 215–221.
10. J. Watton. "The Stability of Electrohydraulic Servomotor Systems with Transmission Lines and Nonlinear Motor Friction Effects. Part A: System Modeling," *The Journal of Fluid Control, including Fluidics Quarterly*, Vol. 16, No. 2-3, 1986, pp. 118–136.
11. S. A. Huckvale, et al. "A Review of the Application of Microprocessors to Electrohydraulic Control Systems," *Proc. IMechE Conference, Microprocessors in Fluid Power Engineering*, IMECHE 1984, C237/84.
12. G. J. Blickley. "Servo Valve Becomes Digital Actuator," *Control Engineering*, June 1986, pp. 76–77.
13. V. I. Utkin. "Variable Structure Systems with Sliding Modes: A Survey," *IEEE Trans. Automatic Contr.*, Vol. AC- 22, No. 2, April 1977, pp. 212–222.

APPENDIX I

Valve Steady-State Model

The flow through the valve is given by the following relation for a positive valve displacement:

$V_x > 0$:

$$Q_1 = CV_x \operatorname{sgn}(P_s - p_1)\sqrt{|P_s - p_1|} \tag{I.1}$$

$$Q_2 = CV_x \operatorname{sgn}(p_2)\sqrt{|p_2|} \tag{I.2}$$

and for a negative valve displacement:

$V_x < 0$:

$$Q_1 = CV_x \operatorname{sgn}(p_1)\sqrt{|p_1|} \tag{I.3}$$

$$Q_2 = CV_x \operatorname{sgn}(P_s - p_2)\sqrt{|P_s - p_2|} \tag{I.4}$$

where V_x is the valve drive voltage, C is the valve coefficient, P_s is the supply pressure, and p_1 and p_2 are the actuator pressures.

Assuming no leakage through the valve, then $P_s = p_1 + p_2$, and defining $P_L = p_1 - p_2$, thus $p_1 = (P_s + P_L)/2$ and $p_2 = (P_s - P_L)/2$. Substituting for p_1 and p_2 from the above relations into the previous flow equations (I.1–I.4), a general form for the valve flow relation can be derived and is given by:

$$Q = K_x V_x \operatorname{sgn}\left[1 - (\operatorname{sgn} V_x)\frac{P_L}{P_s}\right]\sqrt{\left|1 - (\operatorname{sgn} V_x)\frac{P_L}{P_s}\right|} \tag{I.5}$$

where $K_x = C\sqrt{P_s/2}$ is the valve steady-state gain, V_x is the valve input voltage, and P_L is the load pressure.

APPENDIX II

Valve Dynamic Model

A schematic diagram of the valve is given in Figure A. The torque motor produces a torque that is proportional to the armature current, i_x and is given by

$$\tau_m i_x = J_m\ddot{\theta} + B_m\dot{\theta} + K_m\theta + F \tag{II.1}$$

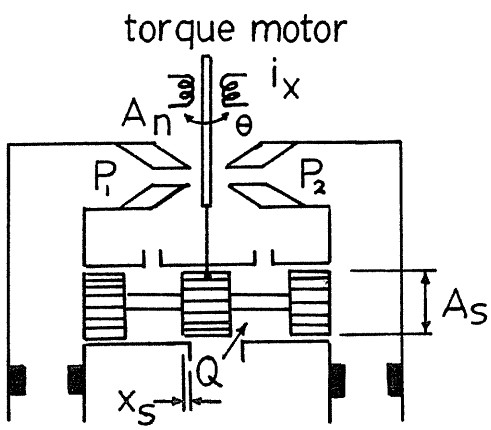

Figure A. Servovalve Model

where τ_m is the torque motor constant, J_m is the flapper inertia, B_m is the flapper viscous friction coefficient, K_m is the flapper restraining spring constant, and F is the flow forces.

Neglecting flapper inertia and viscous friction, Equation II.1 can be approximated as

$$\tau_m i_x = K_m \theta + F \tag{II.2}$$

For linear operation of the torque motor, the instantaneous back flow, i.e., the flow between the nozzle-flapper valve and the spool valve, is given by

$$Q_f = C_n \theta \tag{II.3}$$

where C_n is a constant.

The fluid force on the flapper can be approximated by the static pressure force by neglecting the dynamic flow force and is expressed as

$$F = A_n(p_1 - p_2) \tag{II.4}$$

where A_n is the area of the nozzle.

The instantaneous flow can be interrelated to the input current and load pressure by combining Equations 2, 3 and 4 to give

$$Q_f = \frac{\tau_m C_n}{K_m} i_x - \frac{C_n}{K_m} A_n (p_1 - p_2) \tag{II.5}$$

The equation of motion of the second stage spool is given by

$$(p_1 - p_2)A_s = m_v \ddot{x}_s + B_v \dot{x}_s + K_v x_s \tag{II.6}$$

where A_s is the end area of the spool, m_v is the mass of the spool, B_v is the viscous coefficient, K_v is the equivalent coefficient of the two centering springs and x_s is the spool displacement.

Equation II.6 can be reduced to the following relation upon neglecting spool inertia and viscous force

$$(p_1 - p_2)A_s = K_v x_s \tag{II.7}$$

Substituting Equation II.7 into Equation II.5 gives

$$Q_f = \frac{\tau_m C_n}{K_m} i_x - C_n \frac{A_n}{A_s} \frac{K_v}{K_m} x_s$$

or

$$Q_f = K_f i_x - K_{sf} x_s \tag{II.8}$$

where K_f is the flapper gain and K_{sf} is the spool-flapper feedback constant.

The coupling between the spool displacement, x_s, and the back flow from the first stage is achieved through the continuity equation upon neglecting fluid compressibility and leakage across the spool:

$$Q_f = A_s \dot{x}_s \tag{II.9}$$

Substitution of Q_f from Equation II.9 into Equation II.8, gives

$$\dot{x}_s A_s + x_s K_{sf} = i_x K_f$$

or

$$\frac{A_s}{K_{sf}} \dot{x}_s K_s + x_s K_s = i_x K_f \frac{K_s}{K_{sf}} \tag{II.10}$$

where K_s is the spool gain.

The flow through the spool valve port for constant pressure operation is given by

$$Q = x_s K_s \tag{II.11}$$

Equation II.10 can be equally expressed by the following relation for convenience, upon substituting for Q from Equation II.11.

$$\tau \frac{dQ}{dt} + Q = V_x K_x \tag{II.12}$$

where $\tau = A_s/K_{sf}$ is the valve time constant, Q is the valve flow rate, V_x is the valve drive voltage, and K_x is the steady-state gain of the valve.

Nomenclature

B	Viscous damping coefficient, N·m·s/rad
J	Load inertia, N·m·s^2/rad
K_a	Operational amplifier gain
K_h	Bulk modulus of oil, N/m^2
K_x	Valve steady-state gain at $P_L = 0$, m^3/s/v
k_s	Position transducer constant, v/rad
k_t	Tachogenerator constant, v/rad/s
k_θ	Position feedback gain
k_ω	Velocity feedback gain
L_e	Equivalent leakage coefficient, m^5/N·s
n	Reduction gear ratio
p_1, p_2	Pressures at actuator ports, N/m^2
P_L	Load pressure, N/m^2
P_s	Supply pressure, N/m^2
Q_1, Q_2	Inlet and outlet flow of actuator, m^3/s
Q	Mean flow rate, m^3/s
T_c	Magnitude of Coulomb-friction, N·m
t	Time, s
V_c	Volume of oil in motor and hoses, m^3
V_i	Input voltage to the system (reference input), v
V_m	Motor displacement, m^3/rad
V_x	Valve drive voltage, v
τ	Valve time constant, s
θ	Shaft angular position

Acknowledgment

The authors acknowledge the benefits of discussion with Dr. J. L. Shearer.